Journal of Applied Fluid Mechanics, Vol. 16, No. 12, pp. 2364-2380, 2023.
Available online at www.jafmonline.net, ISSN 1735-3572, EISSN 1735-3645.
https://doi.org/10.47176/jafm.16.12.2028

Fluid Flow and Effect of Turbulence Model on Large-Sized Triple-Offset Butterfly Valve

M. S. Kim[1], H. S. Seong[2], J. H. Yang[3], S. W. Lee[3], and S. W. Choi[†3]

[1]*Korea Railroad Research Institute, Metropolitan Transportation Research Center, Uiwang-si, Gyeonggi-do, Republic of Korea*
[2]*DH Controls Co., Ltd., Research Institute, Gangseo-gu, Busan, Republic of Korea*
[3]*Gyeongsang National University, Department of Mechanical System Engineering, Tongyeong-si, Gyeongsangnam-do, Republic of Korea*

†Corresponding Author Email: younhulje@gnu.ac.kr

ABSTRACT

The performance a valve has been frequently estimated with numerical methods owing to limitations such as cost and place. In this study, for the triple-offset butterfly valves, the different sizes in various disc-opening cases was numerically conducted using different turbulence models of the two-equation turbulence models of k–ε, k-ω, and Reynolds stress model. The numerical calculations were validated against experimentally obtained valve flow test results. The numerical effect with the different turbulence models were analyzed with respect to the disc-opening cases. From the numerical analysis, the Reynolds stress model exhibits the most pronounced turbulence effects among the various turbulence models showing higher value of Reynolds normal stress near the valve disc region. The sensitivity of the turbulence model constants was examined using the 300 mm valve to observe the sensitivity of the turbulence model parameters in the two-equation turbulence models.

Article History

Received May 20, 2023
Revised August 1, 2023
Accepted August 16, 2023
Available online October 8, 2023

Keywords:

Triple-offset butterfly valve
Two-equation turbulence model
Valve flow
Reynolds stress
Turbulence constant

1. INTRODUCTION

Valves have various sizes and configurations to satisfy the performance requirements of fluid systems. Engineering design of valves for their sizes and performances are important because the performance of a fluid system is dependent on their main components such as valves. The performance of a valve has been commonly determined by valve coefficients which are the valve loss, and hydrodynamic torque coefficients, valve flow coefficients, which are usually obtained with numerical methods, because obtaining these factors (Del et al., 2015) by experiments is infeasible owing to limitations of cost and place.

In numerical investigations on designing valves, numerical approaches have been adopted to determine the design factors of valve coefficients, such as the hydrodynamic torque coefficient (Ogawa & Kimura, 1995; Park et al., 2006), flow coefficient (Lisowski & Filo, 2017; Sun et al., 2017), and pressure loss characteristics (Lisowski & Rajda, 2013; Wu et al., 2015). For a numerical approach to design valves, the understanding the flow behavior through a valve is essential. Wang and Liu (Wang & Liu, 2017) performed the study of the unsteady flow behavior in the steam turbine control valve especially for the choked condition through detached eddy simulation (DES) method of the unsteady flow field. The compressible air flow phenomena in a typical puffer chamber were numerically studied by Srikanth and Bhasker (Srikanth & Bhasker, 2009) using computational method.

Numerical calculations in a valve are significantly related with the turbulence model. Turbulence model studies have been conducted with various researchers. Zeng et al (Zeng et al., 2015) performed a numerical study on in control valves using four turbulence models, realizable k-ε, SST, DES to predict the flow pattern. The turbulence models are tested with the growth and separation of the boundary layer, as well as boundary layer reattachment. Du and Gao (Du & Gao, 2013) numerically analyzed a valve system using the control valves by carefully examining the pressure and velocity field, and distribution of turbulence using three turbulence models. Said (Said et al., 2016) investigated the turbulence model effect for the valve disc cases by comparing experimental and numerical results.

As noted above, for the robust design of a valve, a numerical approach based on understanding the flow behavior is essential. One of the important considerations for the numerical approach is the adoption of suitable

Nomenclature

C_μ			
$C_{1\varepsilon}$	turbulence constant	$\bar{u}$	mean average velocity
$C_{2\varepsilon}$			
k	turbulence kinetic energy	$w_1 w_2$	examined constants in sensitivity analysis
$\bar{p}$	mean pressure	Y	nominal valve size
Re_t	turbulence Reynolds number	y/Y	
$\tilde{S}_m$	sensitivity coefficient	Δp	pressure decreases across the valve
u	streamwise flow velocity	**Greek Symbols**	
u_s	flow velocity parallel to the wall	$\alpha, \beta, \beta',$ σ_ω, σ_k	turbulence constants
y	distance to the nearest wall	δ_{ij}	Kronecker delta tensor
x/Y	specific location (x: distance from the valve, Y; nominal valve size)	μ	dynamic viscosity
ΔC_m	increment in the turbulence constant	τ_{ij}	turbulence Reynolds stress
f_μ	wall damping functions	ε	turbulence dissipation rate
P	turbulence production	μ_t	turbulent eddy viscosity
Q	flow rate	ρ	density of the material
S_{ij}	mean velocity strain-rate tensor	ω	specific dissipation rate
t	time	Φ_{ij}	pressure–strain term

turbulence model because it affects the accuracy of the numerical calculation in a valve. In the present numerical study, the most frequently used turbulence models in industrial workplaces were considered: two-equation k − ε model of Launder and Sharma and two-equation k − ω model of Wilcox. Also, the sensitivity of the turbulence model of two-equation k − ε model and k − ω model constants was examined. This is because limited studies on the effects of the constant used in a two-equation turbulence model have been conducted for the fluid flow in valve and pipe system. As for the quantitative evaluation of the effect of the two-equation turbulence constant, the present study represents the first attempt for the numerical study of a triple-offset butterfly valve.

In this study, a numerical study on the fluid flow through triple-offset butterfly valve of different sizes was conducted and the turbulence model effect was examined in various valve disc-opening cases. The numerical method was validated using the experimentally obtained valve flow test results with various sizes. The turbulence model effect and the consequent flow behavior in the valves was analyzed in different opening of disc. The sensitivity of the turbulence model constants was examined using the 300 mm valve to analyze sensitivity of the turbulence model used in the two-equation turbulence model.

2. THEORY

2.1 Turbulence Model of Two-Equation

Two equation turbulence model was considered for the $k-\varepsilon$ model ($k-\varepsilon$ of Launder and Sharma) (Jones & Launder, 1972; Launder & Sharma, 1974; Benton et al., 1996; Wilcox, 2008) and $k-\omega$ model of Wilcox ($k-\omega$ model) (Wilcox, 1998, 2008). In the two-equation $k-\varepsilon$ model of Launder and Sharma (the standard $k-\varepsilon$ model), the transport equations for the turbulence kinetic energy (k) and the dissipation rate (ε) are

$$\frac{\partial(\rho k)}{\partial t}+\frac{\partial}{\partial x_j}\left(\rho u_j\frac{\partial k}{\partial x_j}-\left(\mu+\frac{\mu_t}{\sigma_k}\right)\frac{\partial k}{\partial x_j}\right)=\tau_{ij}S_{ij}-\rho\varepsilon+\varphi_k. \quad (1)$$

$$\frac{\partial(\rho\varepsilon)}{\partial t}+\frac{\partial}{\partial x_j}\left(\rho u_j\varepsilon-\left(\mu+\frac{\mu_t}{\sigma_\varepsilon}\right)\frac{\partial\varepsilon}{\partial x_j}\right)=C_{1\varepsilon}\frac{\varepsilon}{k}\tau_{ij}S_{ij}-C_{2\varepsilon}f_2\rho\frac{\varepsilon^2}{k}+\varphi_\varepsilon. \quad (2)$$

The turbulence constants in the standard $k-\varepsilon$ model are typically five constants which are determined empirically: C_μ, $C_{1\varepsilon}$, $C_{2\varepsilon}$, σ_k, and σ_ε. The explicit wall terms (ϕ_k, ϕ_ε) and near wall damping functions (f_μ) are as follows:

$$f_\mu = exp(-3.4/(1+0.02\,Re_t)^2) \quad (3)$$

$$f_2 = 1-0.3\,exp(-Re_t{}^2),\ Re_t=\frac{\rho k^2}{\varepsilon\mu} \quad (4)$$

$$\varphi_k = 2\mu\left(\frac{\partial\sqrt{k}}{\partial y}\right)^2 \text{ and } \varphi_\varepsilon = 2\mu\frac{\mu_t}{\rho}\left(\frac{\partial^2 u_s}{\partial y^2}\right)^2 \quad (5)$$

where u_s represents the velocity of the flow parallel to the wall.

The $k-\omega$ model with a two-equation eddy viscosity model includes the convective transport equations for turbulence kinetic energy (k) and its specific dissipation rate (ω). The eddy viscosity is determined by the specific dissipation rate (ω) and the turbulence kinetic energy (k), which is expressed as the ratio of the dissipation and turbulence intensities as proposed by Kalitzin et al. (Benton et al., 1996), which was further developed by Wilcox (Wilcox, 1998, 2008) as follows:

$$\mu_t = \rho\frac{k}{\omega} \quad (6)$$

Two transport equations expressed with the turbulence kinetic energy (k) and the specific dissipation rate (ω) are follows:

$$\frac{\partial(\rho k)}{\partial t}+\frac{\partial}{\partial x_j}\left(\rho u_j k-\left(\mu+\frac{\mu_t}{\sigma_k}\right)\frac{\partial k}{\partial x_j}\right)=\tau_{ij}S_{ij}-\beta'\rho k\omega \quad (7)$$

$$\frac{\partial(\rho\omega)}{\partial t}+\frac{\partial}{\partial x_j}\left(\rho u_j\omega-\left(\mu+\frac{\mu_t}{\sigma_\omega}\right)\frac{\partial\omega}{\partial x_j}\right)=\alpha\frac{\omega}{k}\tau_{ij}S_{ij}-\beta\rho\omega^2 \tag{8}$$

2.2 Reynolds Stress Model

The Reynolds stress (RS) model, which is a second-order closure model, can be obtained by solving the following transport equations (Lin et al., 2014) as follows:

$$\frac{\partial}{\partial t}\left(\rho\langle u_i'u_j'\rangle\right)+C_{ij}=D_{\tau,ij}+\frac{\partial}{\partial x_k}\left(\mu\frac{\partial}{\partial x_k}\langle u_i'u_j'\rangle\right)+P_{ij}+\Phi_{ij}-\varepsilon_{ij} \tag{9}$$

Where

$$C_{ij}=\frac{\partial}{\partial x_k}\left(\rho\langle u_k\rangle\langle u_i'u_j'\rangle\right) \tag{10}$$

$$P_{ij}=-\rho\left(\langle u_i'u_k'\rangle\frac{\partial\langle u_j\rangle}{\partial x_k}+\langle u_i'u_k'\rangle\frac{\partial\langle u_i\rangle}{\partial x_k}\right) \tag{11}$$

$$D_{\tau,ij}=-\frac{\partial}{\partial x_k}\left(\frac{\mu_t}{\sigma_k}\frac{\partial\langle u_i'u_j'\rangle}{\partial x_k}\right) \tag{12}$$

The pressure–strain term, Φ_{ij}, reflects the production and transport processes of the Reynolds stresses and plays a fundamental role in shaping the structures of turbulent flows. The pressure-strain term is especially significant when it comes to accurately predicting anisotropic flow characteristics in turbulent flows.

2.3 Turbulence Constants in Two-Equation Models

In the standard $k-\varepsilon$ model, the turbulence constants have been applied by Bottema (Bottema, 1997), Comte-Bellot and Corrsin (Comte & Corrsin, 1966), Hrenya et al. (Hrenya et al., 1995), Launder and Spalding (Launder & Spalding, 1972), and Shih (Shih, 1990).

The values of constants used in the standard $k-\varepsilon$ turbulence models are $C_{\varepsilon1}$ = 1.44, $C_{\varepsilon2}$ = 1.92, C_μ = 0.0900, σ_k = 1.00, and σ_ε = 1.30 (Sarkar & So, 1997). However, the ranges of the constant values are varied in many investigations as shown in Table 1. The values of $C_{\varepsilon1}$, $C_{\varepsilon2}$, C_μ, σ_k, and σ_ε are in the ranges of 1.15 1.50 (Chen and Kim 1987; Hrenya et al., 1995; Sarkar & So, 1997; Sarkar et al. 1997), 1.68–2.00 (Sarkar et al., 1997; Shih et al., 1995), 0.0300–0.0900 (Bottema, 1997; Shih, 1990), 0.500–1.75 (Launder & Spalding, 1972), and 0.610–1.36 (Bottema, 1997), respectively(Błazik, 2008). The values of constants used in the $k-\omega$ turbulence models are the following values (Wilcox, 2008; Shih, 1990) as shown in Table 1: α = 0.556, β = 0.0750, β' = 0.090, σ_k = 2, and σ_ω = 2. However, these constants have been observed to vary over a wide range of values. The values of α, β, β', σ_k, and $\sigma_\omega$are in the ranges of 0.52–0.556 (Wilcox, 2008), 0.075–0.083 (Bardina et al., 1997), 0.09 (Shih et al., 1995; Wilcox, 1998), 1.5–2 (Kok, 2000), and 1.67–2 (Kok, 2000; Wilcox, 2008), respectively. As mentioned above, the turbulence constants used in the two-equation $k-\varepsilon$ and $k-\omega$ models have wide ranges of values. Flows in valves with various disc-opening cases present different geometric characteristics; therefore, flow phenomenon shows different behavior with different turbulence models. The sensitivity of model constants should be examined by adopting various constants in each turbulence model, to accurately predict flow phenomenon by numerical calculations.

Table 1 The ranges of the turbulence constant value

Parameters	results
$C_{\varepsilon1}$	1.15–1.50 [23, 27-29]
$C_{\varepsilon2}$	1.68–2.00 [29-30]
C_μ	0.0300–0.0900 [21, 26]
σ_k	0.500–1.75 [25]
σ_ε	0.500–1.75 [25]
α	0.52–0.556 [19]
β	0.075–0.083 [32]
β'	0.09 [15, 30]
σ_k	1.5–2 [33]
σ_ε	1.67–2 [19, 33]

2.4 Sensitivity of Turbulence Model Constants

In the two-equation $k-\varepsilon$ and $k-\omega$ models, to obtain time-averaged values by Reynolds averaging, the simplified assumptions of the Boussinesq approximation and the Prandtl hypotheses are employed (Patel, 2010). In this study, the constants of turbulence model were used based on these time-averaged assumptions to describe the turbulence. The sensitivity of model constants should be estimated from their effects on the numerical results of each turbulence model. The sensitivity analysis methods of Błazik and Borowa (Błazik, 2008, 2012) and Pelletier et al. (Colin et al., 2005) were adopted in this study. With the streamwise flow velocity (u), turbulence kinetic energy (k), turbulence dissipation rate (ε), turbulent eddy viscosity (μ_t), the main flow properties were described based on the time-averaged values for the two-equation $k-\varepsilon$ turbulence model. With the streamwise flow-velocity (u), turbulence kinetic energy (k), turbulence specific dissipation rate (ω), and turbulent eddy viscosity (μ_t), the main flow properties were also described based on the time-averaged values for the two-equation $k-\omega$ turbulence model.

For the constants of each turbulence model, the sensitivity of flow properties can be examined using sensitivity coefficients, which are determined using the finite difference approximation. The general form of the sensitivity coefficient can be expressed as follows (Błazik 2008, 2012):

$$\tilde{S}_m=\frac{w_2-w_1}{\Delta C_m} \tag{13}$$

where $\tilde{S}_m$, ΔC_m, w_1, and w_2 are the sensitivity coefficient, increment in the examined constants, and calculation results at $C_m-\Delta C_m/2$ and $C_m+\Delta C_m/2$, respectively.

For the flows with the different disc-opening cases, sensitivity analysis of a 300 mm-sized valve was representatively conducted using Eq. 10. For the flow properties, the constants of each turbulence model were as follows: $C_{\varepsilon1}$, $C_{\varepsilon2}$, C_μ, σ_k, and σ_ε for the $k-\varepsilon$ model and α, β, β', σ_k, and σ_ω for the $k-\omega$ model. The increments in the constants of each turbulence model in the sensitivity analysis were as follows: $\Delta C_{\varepsilon1}$, $\Delta C_{\varepsilon2}$, $\Delta\sigma_k$, and $\Delta\sigma_\varepsilon$ = 0.1

Table 2 Specification of triple offset butterfly valve

Parameters	Value
Design pressure [bar]	10
Offset	Triple
Seat	Laminated
Connection	ANSI 150 lb Wafer
Nominal size [mm]	300, 400, 450

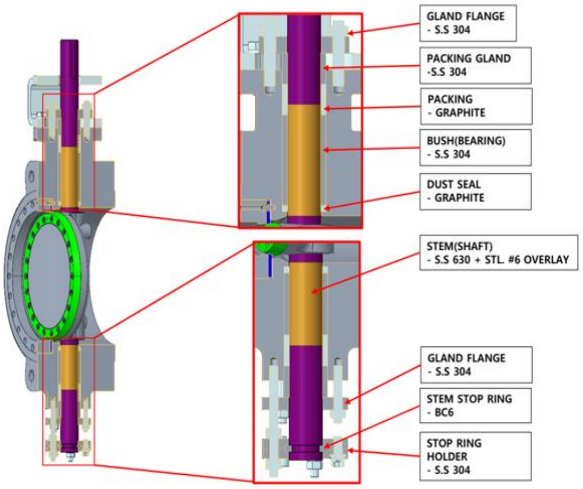

(a)

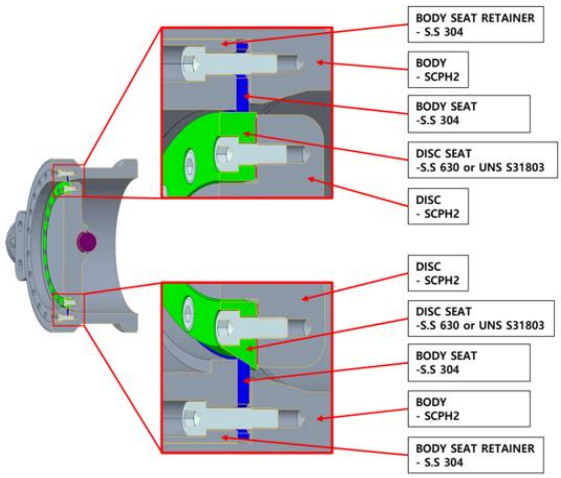

(b)

Fig. 1 Triple Offset Butterfly Valve for numerical calculation (a: Structure of Triple Offset Butterfly Valve, b: Structure of disc and seat)

and ΔC_μ = 0.01(Błazik, 2008, 2012) for the $k-\varepsilon$ model, and $\Delta\alpha$, $\Delta\beta$, $\Delta\beta'$, $\Delta\sigma_k$, and $\Delta\sigma_\omega$ = 0.01 for the $k-\omega$ model (Błazik, 2008, 2012).

3. NUMERICAL IMPLEMENTATION

In the numerical formulation in this study, triple-offset butterfly valves of different sizes were considered, and the specifications of each valve are provided in Table 2. A triple-offset butterfly valve broadly consists of a stem, disc, and body, as shown in Fig. 1. The packing and seat components were formed between the stem and the body and the body and the disc, respectively. Numerical studies involving different turbulence models are conducted, and their accuracies were evaluated by comparing the results obtained from each model.

3.1 Governing Equations

The governing equations for the turbulent fluid flow are based on the principles of conservation of mass and momentum. The Reynolds-averaged Navier-Stokes (RANS) equations consider the time-averaged flow properties and incorporate turbulence models to account for the effects of turbulence on the mean flow field.

The conservation equations of mass and momentum are as follows:

$$\frac{\partial \rho}{\partial t}+\frac{\partial}{\partial x_i}(\rho\overline{u_i})=0 \tag{14}$$

$$\frac{\partial}{\partial t}(\rho\overline{u_i})+\frac{\partial}{\partial x_j}(\rho\overline{u_i u_j})=-\frac{\partial \overline{p}}{\partial x_i}+\frac{\partial}{\partial x_j}\left(\mu\left(\frac{\partial \overline{u_i}}{\partial x_j}+\frac{\partial \overline{u_j}}{\partial x_i}\right)+\tau_{ij}\right) \tag{15}$$

where the velocity components in the x_i direction are represented by u_i (where i can take the values 1, 2, or 3). The other components of p, ρ, τ_{ij}, and δ_{ij} are the pressure, density, turbulence Reynolds stress and Kronecker delta tensor, respectively.

The Reynolds stresses in the RANS equations can be expressed by Reynolds averaging, an eddy viscosity model, and the Boussinesq hypothesis for modeling the Reynolds stresses in turbulent flows (Jones & Launder, 1972; Launder & Sharma, 1974; Benton et al., 1996; Wilcox, 1998) as follows:

$$\tau_{ij}=-\rho\overline{u_i u_j}=\breve{u}\left(\frac{\partial U_i}{\partial x_j}+\frac{\partial U_j}{\partial x_i}\right)-\frac{2}{3}\rho k\delta_{ij} \tag{16}$$

where k and $\breve{\mu}$ represent the turbulence kinetic energy and eddy viscosity, respectively. The mean velocity components are denoted by U_i (where i can take the values $1, 2, \text{or } 3$). The use of the over-bar is stated to indicate time averaging.

3.2 Experimental Conditions Of Flow Test

Measurement of the flow coefficient in valve design is one of the widely used practical methods (Williams et al., 2006) because the flow coefficient is regarded as the valve capacity. The flow coefficient is experimentally measured for the three different diameters of triple-offset butterfly valves of 300 mm (12 inch), 400 mm (16 inch), and 450 mm (18 inch) diameters by ISA standard S75.01, 02 (ISA 2007a; ISA 2007b) where a valve flow coefficient is measured as the quantity of water that flows through the valve per minute at a temperature of 60 °F(Fahrenheit) under a pressure drop of 1 psi (pound per square inch) (ISA 2007a; ISA 2007b). Flow condition was controlled with two throttle valves located with upstream and downstream, and pressure and flow volume were obtained by pressure and flow meters as shown in Fig. 2. The measured flow data is averaged data, because the flow measurements have been time-averaged over a certain period or region. For triple-offset butterfly valves, the flow coefficient (Cv) is typically measured under the condition of 100% valve opening. This means that the valve is fully open when the flow coefficient is determined.

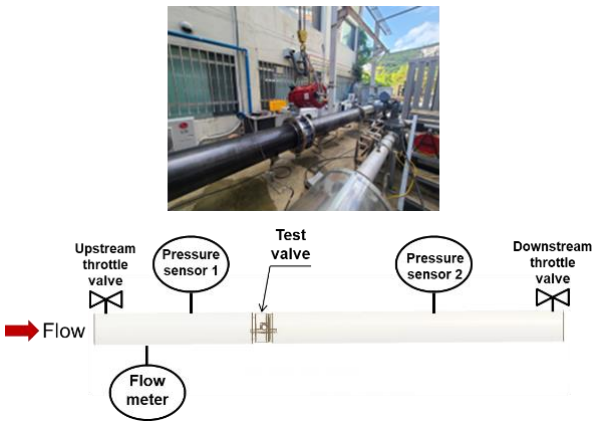

Fig. 2. Experimental setup for the flow coefficient measurement.

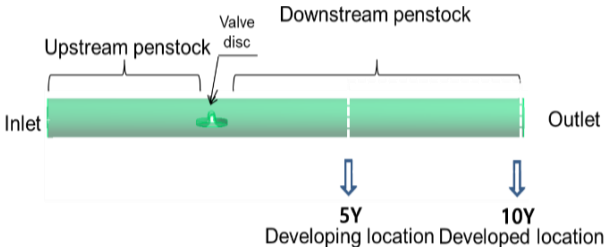

Fig. 3 Triple Offset Butterfly and connected pipe

Table 3 Numerical calculation conditions

Valve size [mm]	Inlet pressure [kPa]	Outlet pressure [kPa]
300	6.90	atmospheric
400	27.2	20.4
450	69.2	62.5

3.2 Calculation Conditions

A representative cross-section of a triple-offset butterfly and pipe is shown in Fig. 3. The distances from the valve necessary for the flow to fully develop, which are the upstream and downstream lengths, were five and ten times the pipe diameter (Huang & Kim, 1996). For the calculation of the performance of three different valves, distinct inlet pressure conditions were considered as boundary conditions, operating under a consistent pressure drop of 1 psi, in accordance with the experimental conditions shown in Table 3. Water was selected as the working fluid with 999 kg/m^3 density and 1.12x10^{-3} N·S/m^2 dynamic viscosity. It is assumed that the flow was a three-dimensional flow, and the fluid was considered incompressible and steady. At the surfaces of the pipe and valve disc, non-slip boundary conditions were applied. For the meshing process, the hexahedral elements and a structured hexahedral non-adaptive grid with 300,000 nodes is generated with the grid generation process. For the near-wall flow model, a maximum y+ of 20 at the valve surface and the pipe wall was considered, referring to the research by Launder and Spalding (Launder & Spalding, 1972). To ensure smooth convergence during numerical simulations, the convergence criteria used during each time step were based on the velocity, mass, and energy balance residuals, with values set below 10^{-4}, 10^{-6} and 10^{-6}, respectively. Numerical calculations are conducted using the finite volume method within a commercial CFD (Computational Fluid Dynamics) package, ANSYS-CFX.

4. RESULTS AND DISCUSSION

4.1 Mesh Independence Analysis

Mesh independence analysis was examined within the current numerical approach, with a specific focus on evaluating the mesh independence of the numerical results for the valve coefficient using various mesh size increments. The investigation focuses on the flow coefficient result for a 300 mm butterfly valve. The analysis establishes a converging criterion by requiring the numerical solutions obtained on different grids to demonstrate agreement within a tolerance level of 0.001. To achieve this convergence, a structured grid approach is employed, progressively increasing the cell size through a coarse grid with 150,000 meshes, a medium grid with 200,000 meshes, and a fine grid with 250,000 meshes. Incremental increases in the number of mesh elements, N, are made while ensuring that skewness and aspect ratio violations are avoided, ultimately identifying the point at which the solution achieves independence from the mesh density. The results, presented in Fig. 4 and Table 4, illustrate a decreasing variation in the solution as the cell size increases. Based on the analysis, a mesh resolution of approximately around 300,000 meshes is selected for the present study, ensuring mesh independence and reliable numerical results for the evaluation of the valve coefficient.

$$\epsilon = \frac{1}{N}\sum_{1}^{N}\left(\sqrt{\left|\frac{X_{coarse}-X_{fine}}{X_{fine}}\right|^2}\right) \quad (14)$$

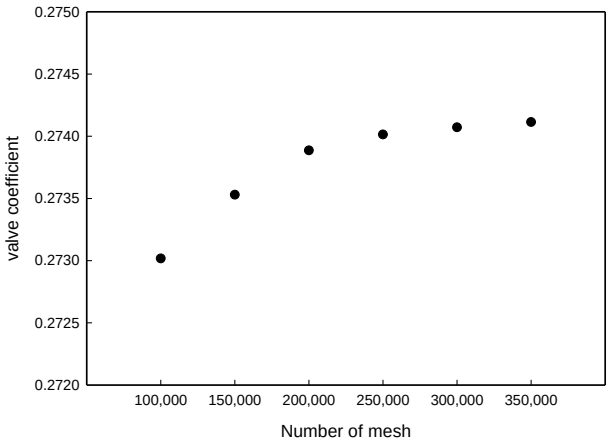

Fig. 4 Mesh independence study for the valve coefficient

Table 4 Mesh independence result

Variables	ϵ for valve coefficient
ϵ grid (coarse-medium)	0.146×10^{-2}
ϵ grid (medium-fine)	0.365×10^{-3}

(fine grid with 250,000 meshes)

Variables	ϵ for valve coefficient
ϵ grid (coarse-medium)	0.365×10^{-3}
ϵ grid (medium-fine)	0.182×10^{-3}

(fine grid with 300,000 meshes)

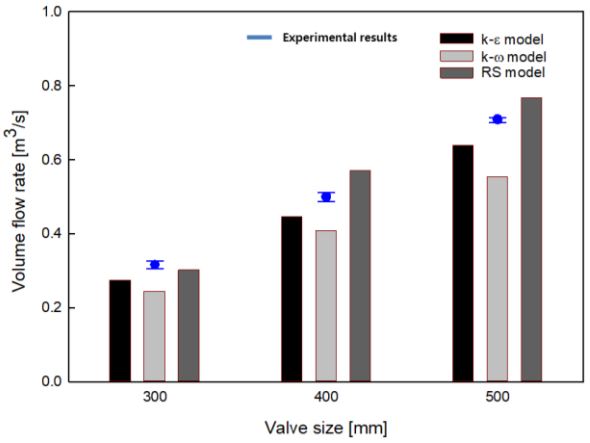

Fig. 5 Predicted flow of valves with different sizes using different turbulence models and experimental results

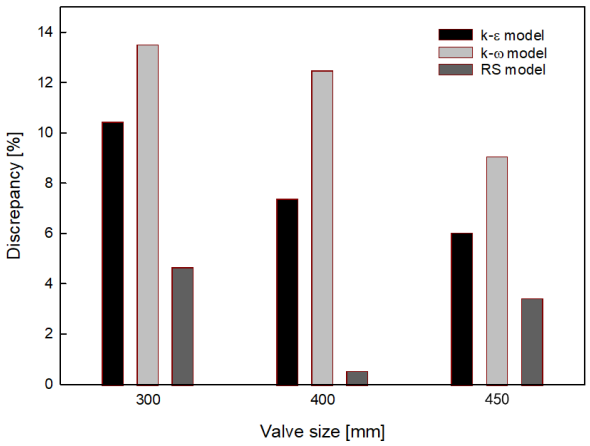

Fig. 6 Discrepancies in flow coefficients of valves of different sizes obtained using different turbulence models

4.2 Numerical Validation with Flow Test Results

The flow in a valve is an important parameter to determine its ability to control the desired flow. It is also a measure of the valve capacity based on the size. In a numerical approach, computation of the flow behavior in a valve is important, which is dependent on the turbulent model. Moreover, choosing the adequate turbulence model is essential to obtain reasonable flow results valve. In this study, the numerical calculations were validated using the experimentally measured flow coefficients of with valves of various sizes. Numerical turbulence model in the valve is validated with Specifically, the experimentally measured flow coefficients of three valves of 300 mm (12 inch), 400 mm (16 inch), and 450 mm (18 inch) diameters were used to validate the k–ε, k–ω, and RS models.

Figures 5-6 shows the predicted flow of valves with different sizes using different turbulence models and experimental results. It can be seen that the discrepancy between the numerical and experimental results is different for different valves. This discrepancy decreases with increasing size of the valve. For the 300 mm-sized valve, the discrepancy is 5–13%. However, as the valve size increases to 450 mm, the discrepancy becomes 3–9 %.

Overall, the RS model shows a low level of discrepancy, indicating high numerical prediction accuracy among the turbulence models. The two-equation k–ε and k–ω models result in 6–10% and 9–13% discrepancies, respectively, showing that the k–ε model is more accurate than the k–ω model. For the 300 mm-sized valve, the flow coefficient is underestimated by all turbulence models compared to the experimental value. However, for the 400 mm and 450 mm-sized valves, the flow coefficients are overestimated by the RS turbulence model and underestimated by the k–ε and k–ω models. This suggests that the flow coefficient is dependent on the flow geometry, which determines the effective flow region to control the flow behavior in a valve.

4.3 Effect of Turbulence Model and Flow Behavior

The effect of the turbulence model and the consequent flow behavior through a valve were numerically investigated, where the flow was influenced by the flow geometry given by the opening angle of the disc and the valve size. Fig. 7 show the velocity contours of different opening angles for the 300 mm, 450 mm valves obtained with the two-equation k–ε and k-ω models in comparison with the RS model results.

Overall, the flow in the valves is observed to develop with vortices and eventually dissipate with a pair of swirling vortices after passing around the valves. The flow stream remains constant until it approaches a valve in the upstream region. The flow through the passing valve varies with increasing velocity owing to the decreased area between the disc and the valve wall resulting in highly turbulent flows, including many vortices. After passing the disc, the streamlines along the valve disc are separated, causing significant turbulent and swirling behavior (Henderson et al., 2008). Henderson et al. (Henderson et al., 2008), Del Toro (Del et al., 2015) and our previous works (Choi & Kim, 2020; Choi et al., 2021) reported similar results of turbulence and a pair of vortices. Pairs of swirling vortices with different mixing behaviors for the different opening angles of the disc are observed with an eventual constant flow stream in the downstream region.

As shown in Fig. 8, with the different opening angles of the disc, the flows through the valves exhibit characteristic behaviors at two characteristic locations: a developing location at 5Y and the developed location at 10Y where Y represent the nominal valve size.

With Fig. 7 and Fig. 9, the small disc opening of 20%, at the 5Y location, vortices are generated at the lower side behind the valves owing to the high level of flow disturbance induced by the high turbulence. After this point, the vortices weakened owing to flow mixing, resulting in a reattachment point of the flow. Flow recirculation existed with flow mixing, and a secondary flow was developed downstream. With developed flow at the 10Y location, each flow was mixed to form a fully developed flow. Among the turbulence models, the RS model best reflected the turbulence effect. A higher turbulence kinetic energy was better expressed by the k–ε model with the two-equation turbulence models as shown in Fig. 10; therefore, the swirling generation was relatively better observed with it.

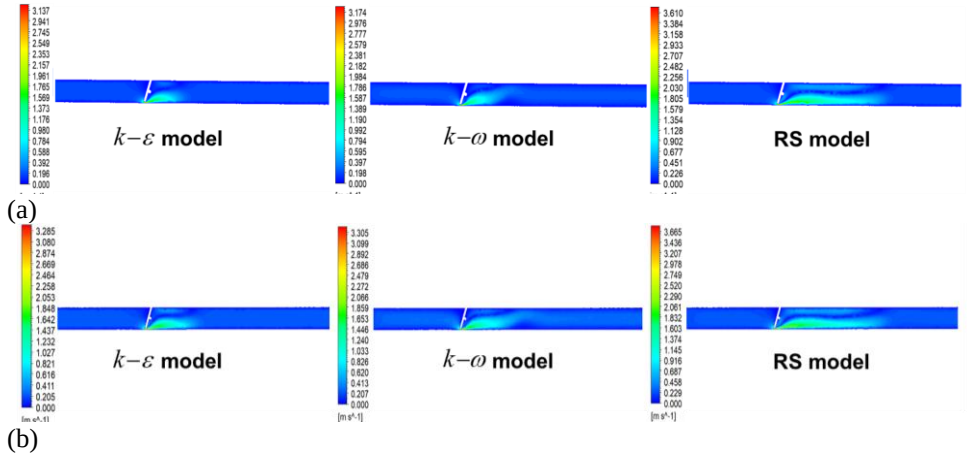

(20% disc opening case)

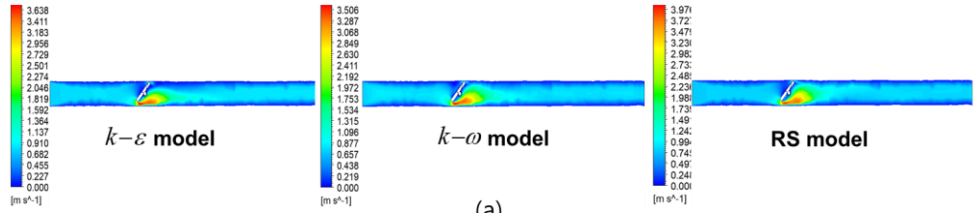

(a)

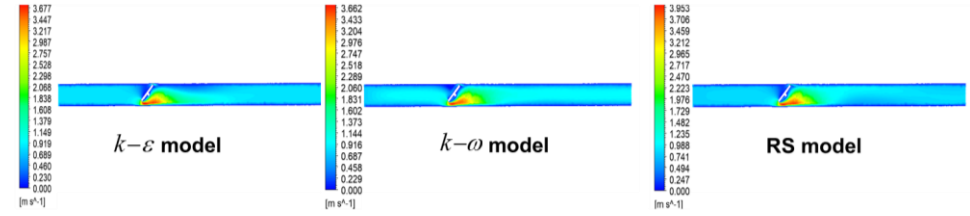

(50% disc opening case)

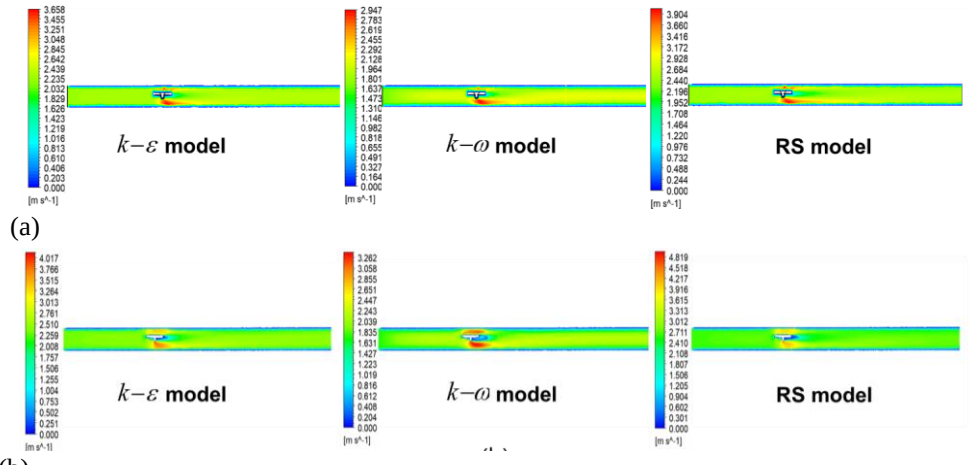

(100% disc opening case)

Fig. 7 Velocity streamline contours in 20-, 50-, and 100%-disc opening case obtained using different turbulence models: (a) 300 mm, (b) 450 mm sized valve

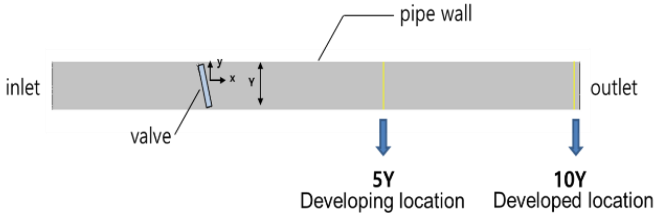

Fig. 8 Two characteristic locations

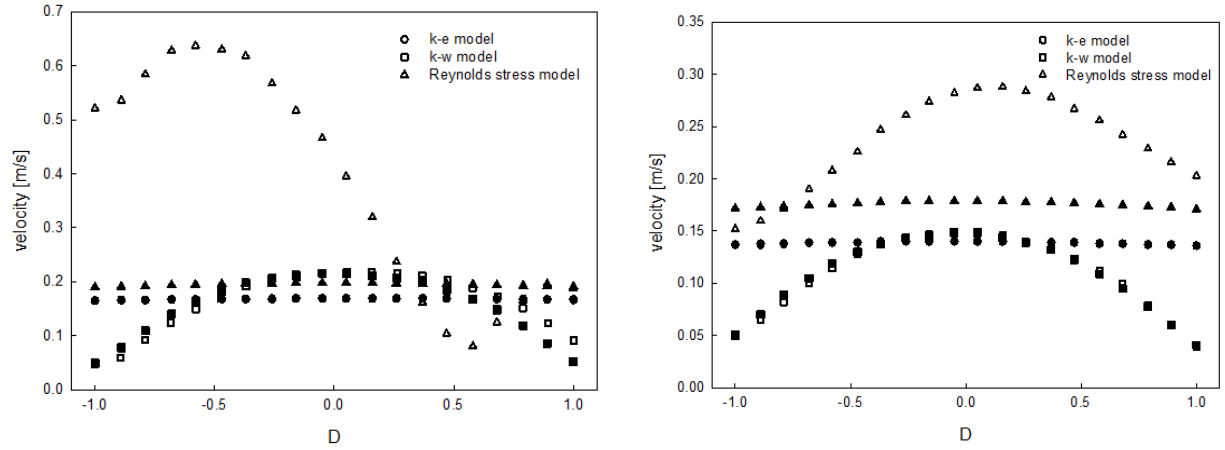

(a) (b)

Fig. 9 Velocity profile with disc opening of 20% at two characteristic locations (a) 300 mm, (b) 450 mm sized valve (open white: 5Y location, closed black: 10Y location)

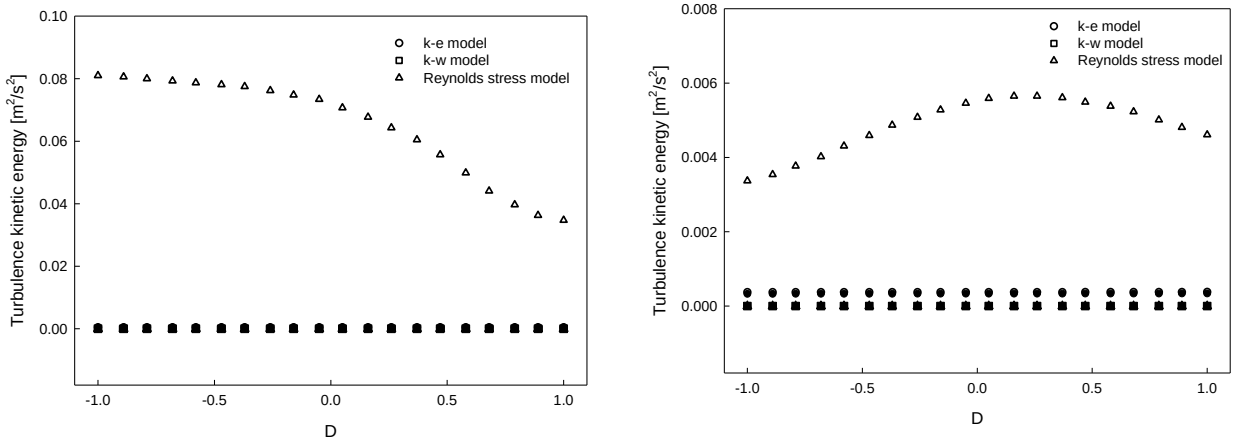

(a) (b)

Fig. 10 Turbulence kinetic energy profile with disc opening of 20% at two characteristic locations (a) 300 mm, (b) 450 mm sized valve (open white: 5Y location, closed black: 10Y location)

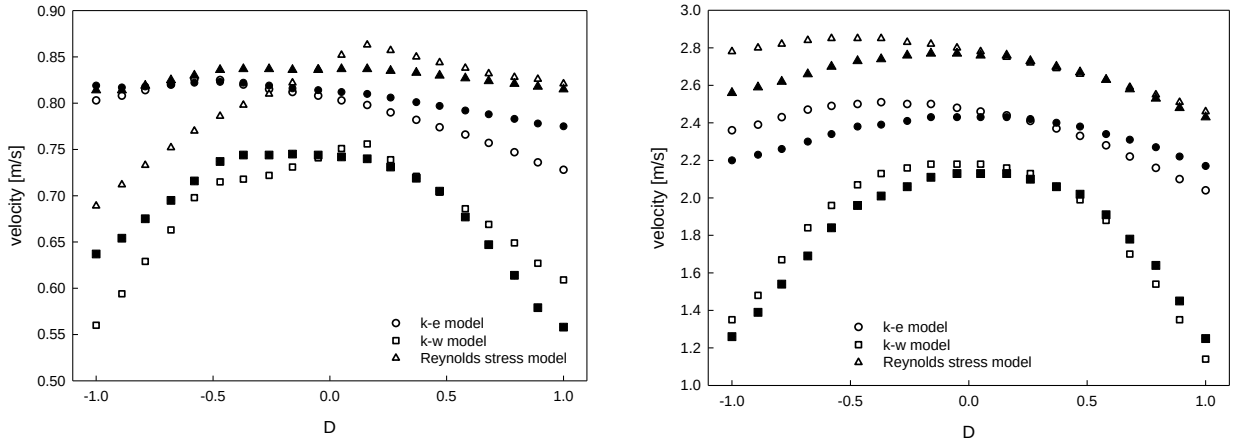

(a) (b)

Fig. 11 Velocity profile at two characteristic locations (a) 300 mm sized valve with disc opening of 50%, (b) 450 mm sized valve with disc opening of 100%, (open white: 5Y location, closed black: 10Y location)

With Fig. 7 and Fig. 11, 50% disc opening, flow recirculation was observed due to the increasing flow passing through the area between the disc and the pipe wall. The flow recirculation was in the form of mixing of vortices resulting from flow wakes. The wake region was in the form of mixing of vortices. At the 5Y location, high turbulence kinetic energy was obtained using the RS model and followed by the k–ε model as shown in Fig. 12. Flow mixing, secondary flow, vortices were developed using the k–ε model than using the k–ω model. At the 10Y location, owing to the significant flow in the gap, the velocity profile was fully developed in

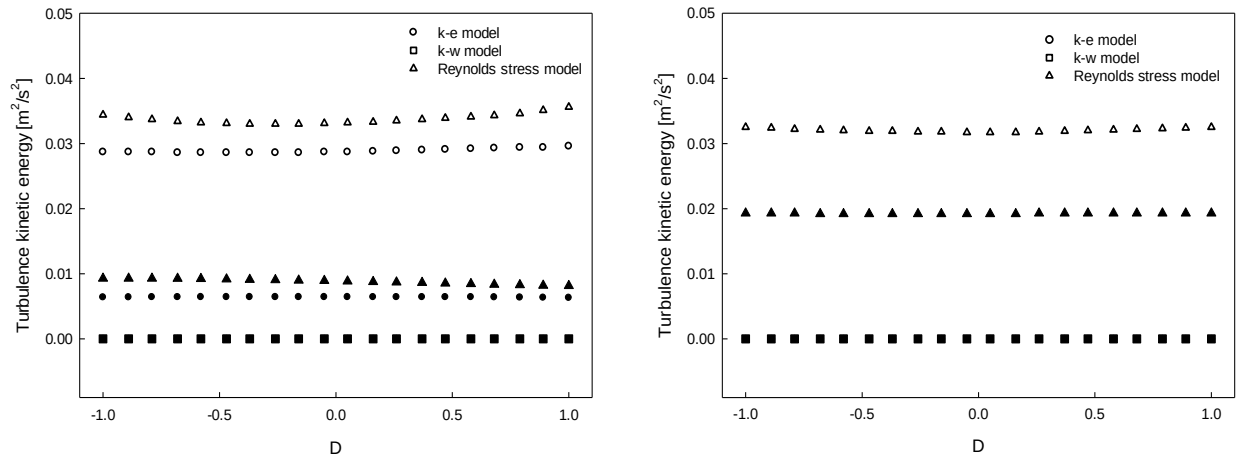

Fig. 12 Turbulence kinetic energy profile at two characteristic locations (a) 400 mm sized valve with disc opening of 50%, (b) 400 mm sized valve with disc opening of 100%, (open white: 5Y location, closed black: 10Y location)

the downside direction, particularly for the 450 mm-sized valve.

With Fig. 7 and Fig. 11, a full opening of 100%, the recirculation and swirling behind each valve were observed to decrease owing to the large area between the disc and the pipe wall. Separate streamwise secondary flows were developed at a point close to the valve disc and flowed in the downstream direction in a reasonably smooth manner. However, in the vortex region, with the appearance of eddies, they rapidly dissipated downstream. Two streamwise secondary flows on the two sides of the valves combined and significantly developed with vortices in the downside direction. In the full opening case, overall, a high turbulence kinetic energy was expressed well by the k–ε model regardless of the location, even better than by the RS model.

Using the different turbulence models, different characteristics of flow behavior were observed, particularly at the 5Y location, with the variation in the valve size and opening angle of the disc. With decreasing valve size and opening angle of the disc, the relatively reduced effective flow region between the disc and the wall increased the pressure drop and the velocity, thereby increasing the turbulence. Among the turbulence models, the RS model expressed the turbulence effect the most. Among the two-equation turbulence models, the k–ε model showed a high level of turbulence kinetic energy better than the k–ω model.

Figure 13 shows that the Reynolds normal stress obtained using the RS model are higher at the 5Y location than 10Y location. It means that the RS model predicts stresses better near the disc region than other region, where isotropic Reynolds stresses are dealt with. However, it requires greater computational effort and cost to solve six additional transport equations to calculate the Reynolds stress than two-equation turbulence models (Prieler et al., 2015). Between the two turbulence models, a high level of turbulence kinetic energy is better expressed by the k–ε model than by the k–ω model; therefore, the former expresses the turbulence effect better.

4.4 Sensitivity of Turbulence Model Constants

The sensitivity of the turbulence model constants was investigated using the sensitivity coefficients obtained from Eq. 10 for the flow behavior in the 300 mm valve at different opening angles of the disc. Four flow properties (streamwise flow velocity, turbulence kinetic energy, turbulence dissipation rate, turbulent eddy viscosity) for five parameters of the two-equation standard k–ε and k–ω models were investigated by conducting a sensitivity analysis.

Figure 14 present the representative results of sensitivity analysis of streamwise flow velocity for the 20, 50, and 100% disc-opening cases. Flow properties at the developing location (5Y) and developed location (10Y) were analyzed.

Table 5 showed the maximum absolute value of sensitivity analysis where the four flow properties (streamwise flow velocity, turbulence kinetic energy, turbulence dissipation rate, turbulent eddy viscosity) was examined for five parameters ($C_{\varepsilon 1}, C_{\varepsilon 2}, C_{\mu}, \sigma_k, \sigma_{\varepsilon}$) of the two-equation standard k–ε and Table 6 showed the maximum absolute value of sensitivity analysis where the four flow properties (streamwise flow velocity, turbulence kinetic energy, turbulence specific dissipation rate, turbulent eddy viscosity) was examined for five parameters ($\alpha, \beta, \beta', \sigma_k, \sigma_{\omega}$) of the two-equation standard and k–ω model.

The results show that the flow properties have differently influenced in the turbulence parameters depending of the opening angle. For the two-equation k–ε model, the flow property most sensitive to the parameters is the turbulence dissipation rate, as shown in Table 5. The turbulence dissipation rate is mainly affected by constants C_{1e} and C_{2e}. At the developing location of 5Y, relatively higher turbulence dissipation rates are observed than location of 10Y, particularly for the low opening of 20%. Extremely high turbulence dissipation rates are observed to be affected by constant C_{1e}. However, at the developed

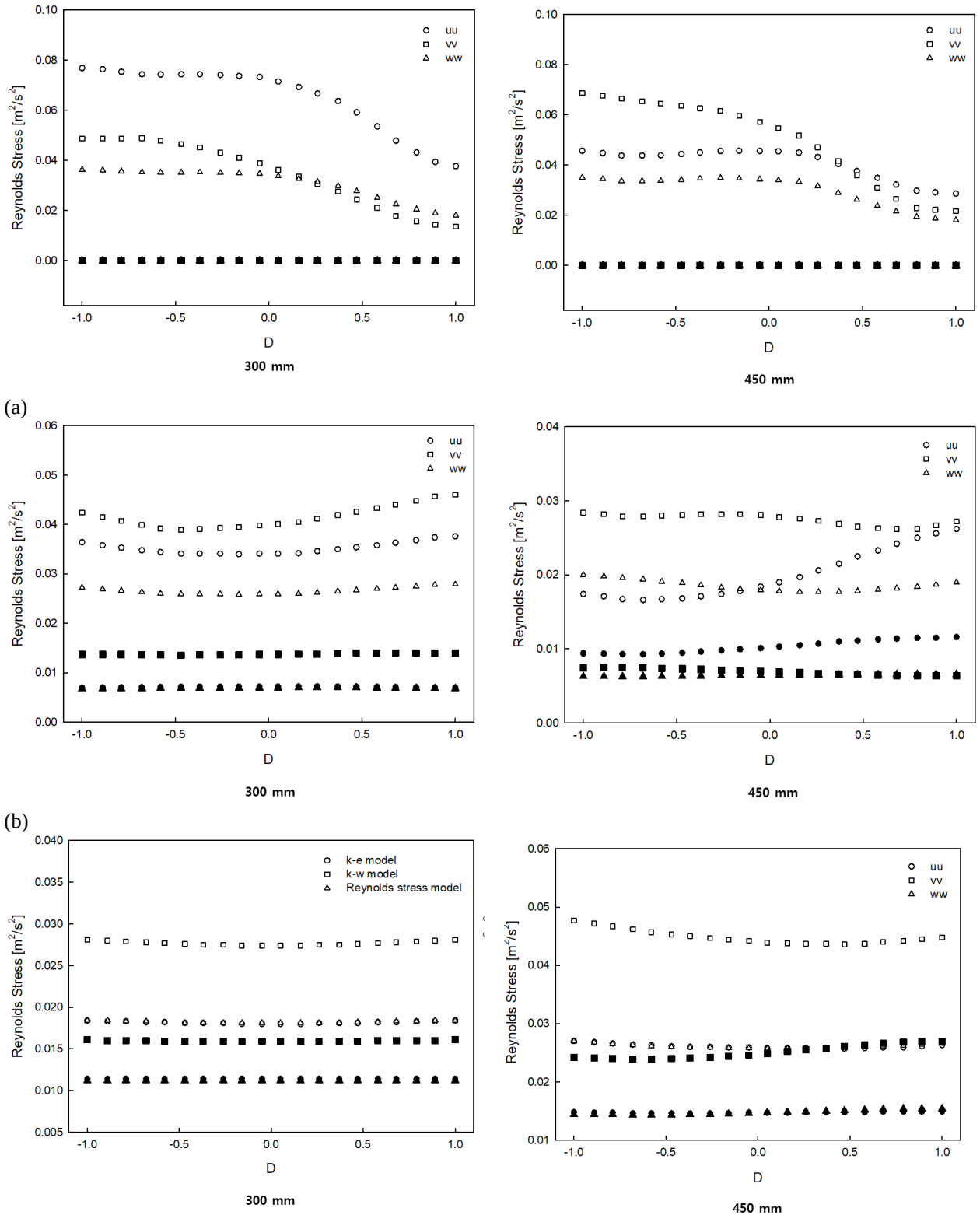

Fig. 13 Reynolds normal stress at two characteristic locations (a) disc opening of 20%, (b) disc opening of 50%, (c) disc opening of 100% (open white: 5Y location, closed black: 10Y location)

location of 10 Y, high turbulence dissipation rates and turbulent eddy viscosity are observed on increasing the opening to 100%. The extremely high turbulence dissipation rates are affected by constants C_{1e} and C_{2e}. This suggests that large discrepancies in the turbulence parameters occur close to the valve disc in the developing and developed flow region with small and large opening angles of the disc, respectively.

For the two-equation $k-\omega$ model also, the flow property most sensitive to the parameters is the turbulence specific dissipation rate, as shown in Table 6. The turbulence dissipation rate is mainly affected by

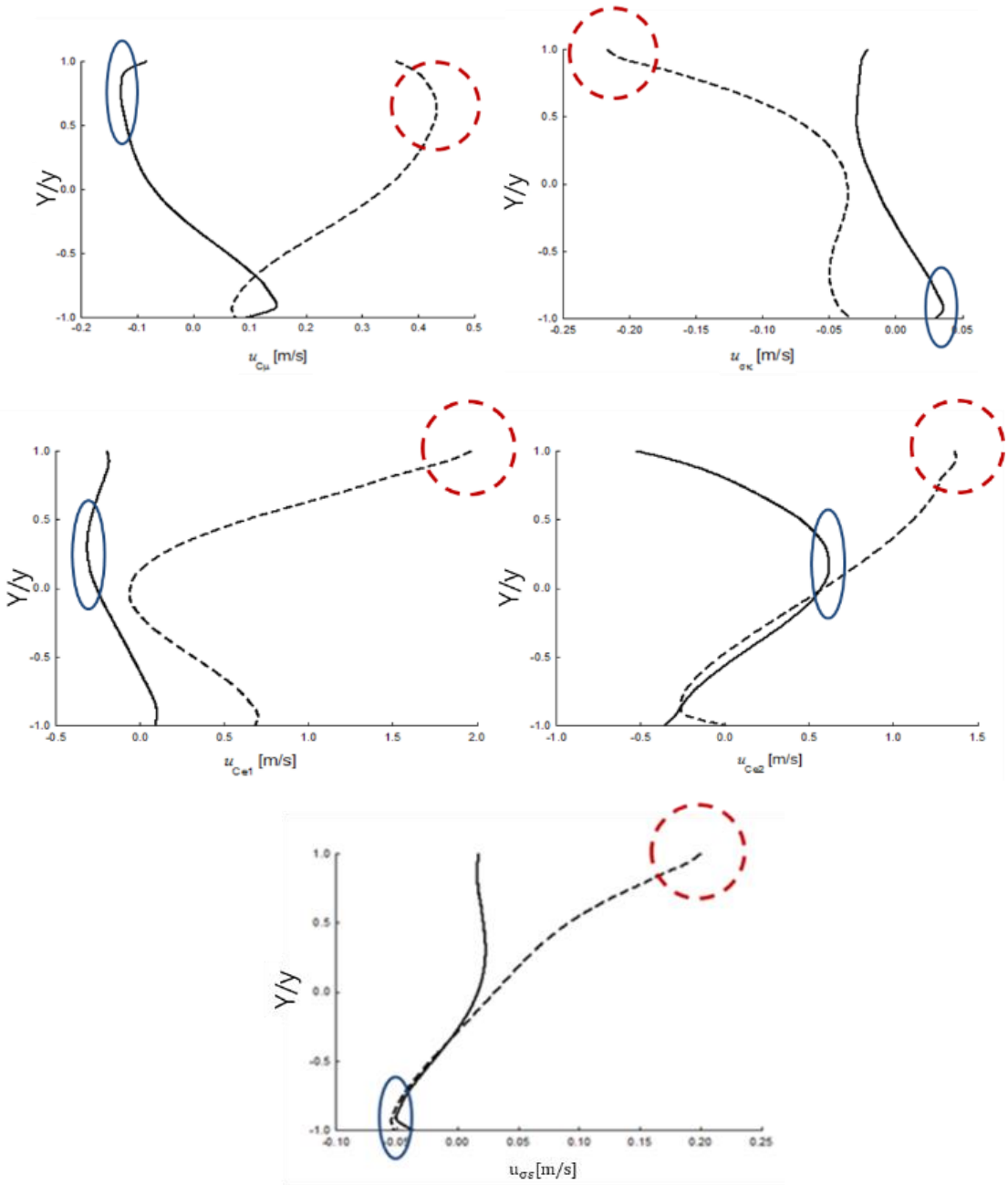
Y/y
$u_{C\mu}$ [m/s]
$u_{\sigma k}$ [m/s]
u_{Ce1} [m/s]
u_{Ce2} [m/s]
$u_{\sigma\varepsilon}$[m/s]

(a)

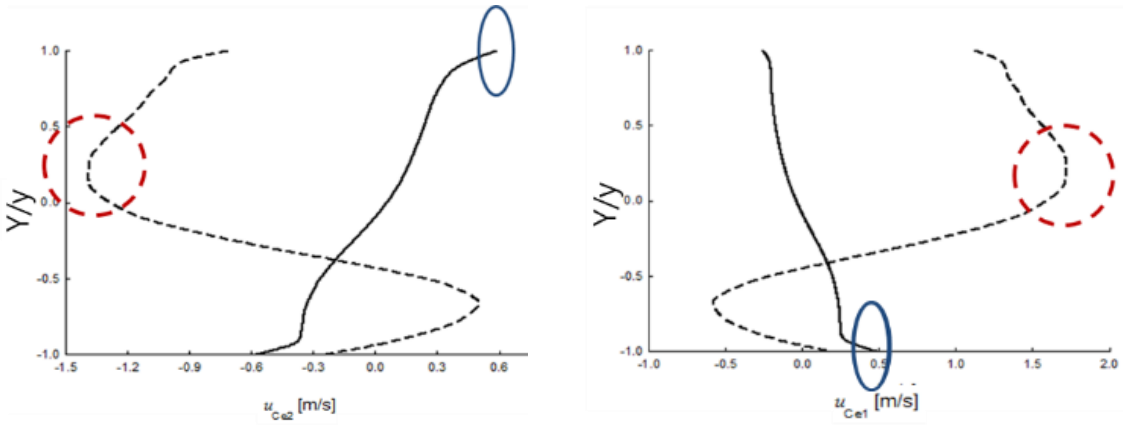
Y/y
u_{Ce2} [m/s]
u_{Ce1} [m/s]

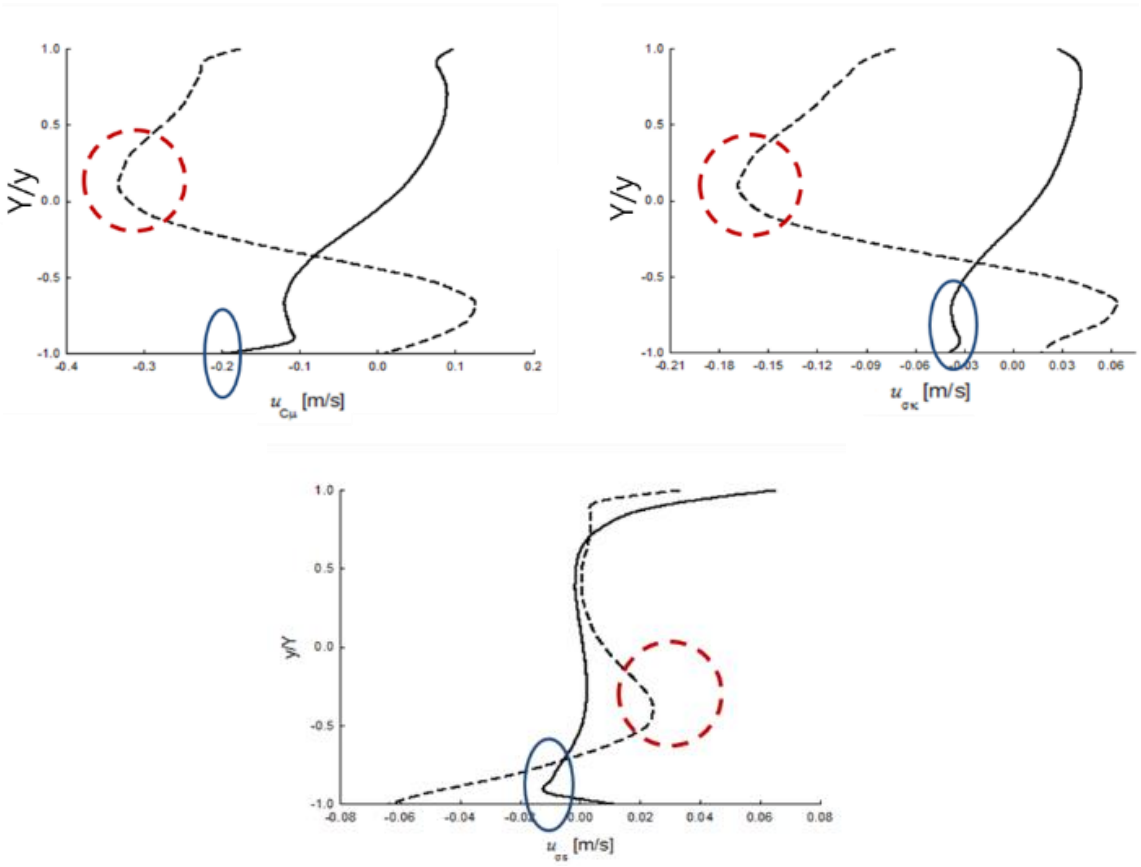
Y/y
$u_{C\mu}$ [m/s]
$u_{\sigma\kappa}$ [m/s]
y/Y
$u_{\sigma\varepsilon}$ [m/s]

(b)

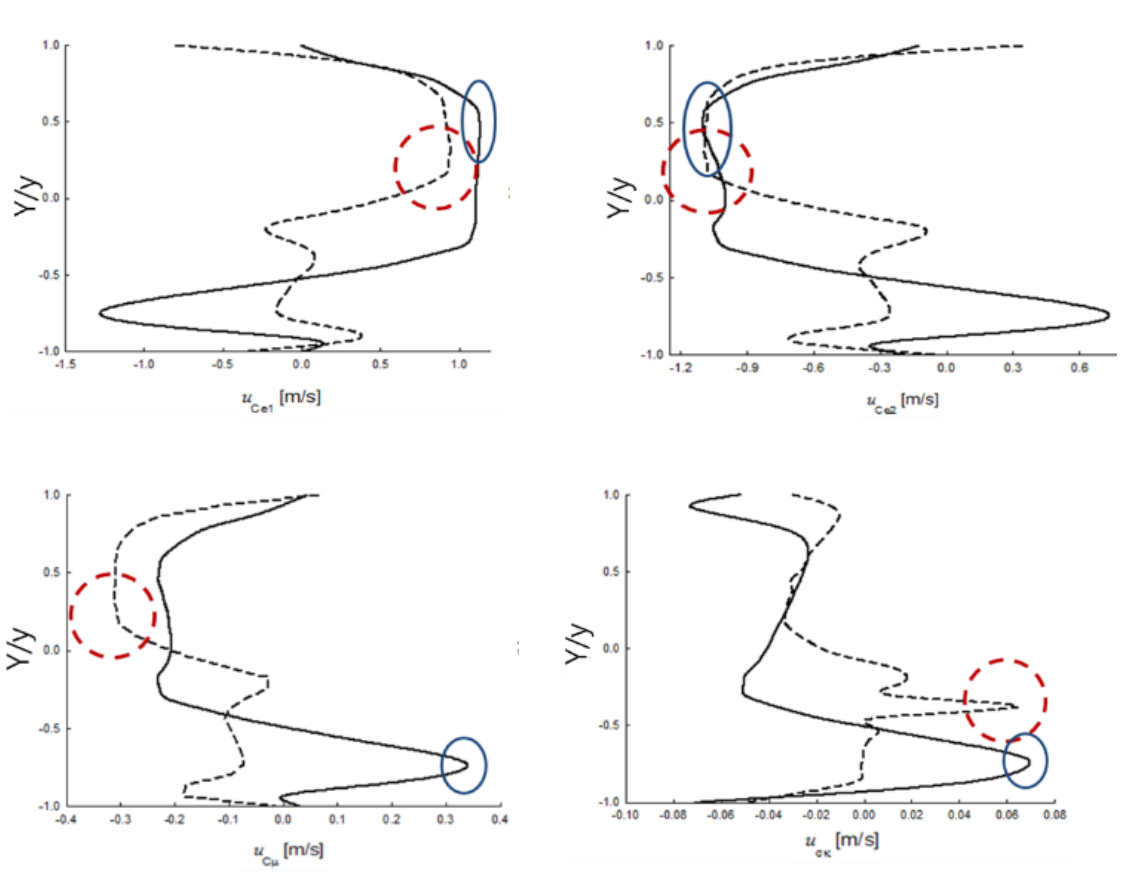
Y/y
u_{Ce1} [m/s]
u_{Ce2} [m/s]
$u_{C\mu}$ [m/s]
$u_{\sigma\kappa}$ [m/s]

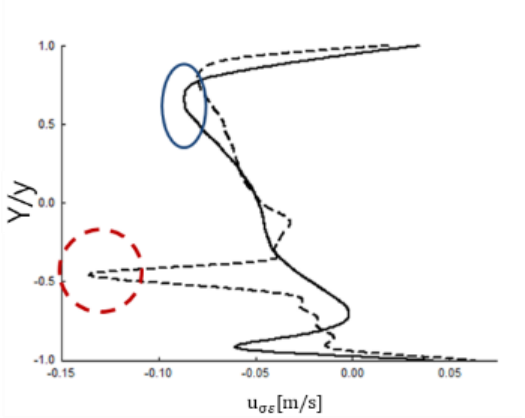

(c)

Fig. 14 Representative results of sensitivity coefficients of streamwise flow velocity with disc opening of (A) 20%, (B) 50% (B) 100% using two-equation k–ε model (Dash line: 5Y location, solid line: 10Y location, extreme values are shown in circles)

Table 5 The results of sensitivity coefficients for the ① Streamwise flow velocity (u), ② Turbulence kinetic energy (k), ③Turbulence dissipation rate (ε), ④ Turbulent eddy viscosity (μ_t) with disc opening of 20%, 50%, 100% using two-equation k–ε model (Values in BOLD represent maximum absolute)

% disc opening		$C_{1\varepsilon}$		$C_{2\varepsilon}$		C_μ		σ_k		σ_ε	
20%	①	**2.16**	0.07	1.51	0.29	0.48	0.08	0.04	0.24	0.22	0.06
	②	**0.65**	0.10	0.41	0.11	0.10	0.12	0.05	0.02	0.02	0.04
	③	**9.00**	1.53	5.38	4.73	0.59	1.93	0.01	0.42	0.36	0.94
	④	0.88	2.23	**4.15**	0.02	0.84	0.12	0.65	0.02	0.21	0.23
50%	①	**1.89**	0.63	0.55	1.53	0.14	0.37	0.07	0.19	0.04	0.07
	②	**0.33**	0.02	0.31	0.01	0.02	0.10	0.03	0.00	0.03	0.01
	③	**7.78**	3.05	1.45	5.12	0.49	1.46	0.19	0.28	0.15	0.40
	④	0.64	1.85	**2.59**	0.21	0.69	0.01	0.49	0.00	0.09	0.01
80%	①	1.04	0.88	**1.20**	0.37	0.07	0.34	0.07	0.05	0.07	0.15
	②	0.01	**0.39**	0.31	0.02	0.05	0.03	0.02	0.02	0.01	0.00
	③	0.61	**5.43**	4.53	0.57	0.93	0.39	0.17	0.19	0.29	0.02
	④	0.01	**2.21**	1.76	0.02	0.50	0.01	0.09	0.07	0.07	0.00

Developing location (5Y)

% disc opening		$C_{1\varepsilon}$		$C_{2\varepsilon}$		C_μ		σ_k		σ_ε	
20%	①	0.11	0.35	**0.68**	0.58	0.16	0.14	0.04	0.03	0.03	0.05
	②	0.00	0.01	**0.28**	0.00	0.00	0.00	0.00	0.00	0.00	0.00
	③	0.09	0.26	0.55	**0.96**	0.02	0.01	0.02	0.00	0.00	0.09
	④	0.06	0.35	0.18	**2.46**	0.09	0.03	0.15	0.09	0.06	0.03
50%	①	0.53	0.28	**0.64**	0.64	0.11	0.22	0.05	0.04	0.07	0.01
	②	0.06	0.01	**0.28**	0.02	0.00	0.03	0.00	0.00	0.01	0.00
	③	**1.31**	0.38	0.60	0.94	0.06	0.34	0.05	0.07	0.17	0.03
	④	0.56	0.32	0.23	**0.95**	0.14	0.09	0.00	0.20	0.10	0.01
80%	①	1.25	**1.37**	0.79	1.21	0.37	0.25	0.08	0.08	0.05	0.10
	②	0.09	**0.33**	0.30	0.04	0.02	0.03	0.01	0.00	0.01	0.00
	③	3.61	**8.20**	2.91	0.86	0.13	0.70	0.44	0.20	0.29	0.24
	④	0.03	2.68	**3.41**	0.05	0.61	0.01	0.17	0.04	0.08	0.01

Developed location (10Y)

Table 6The results of sensitivity coefficients for the ① Streamwise flow velocity (u), ② Turbulence kinetic energy (k), ③Turbulence specific dissipation rate (ω), ④ Turbulent eddy viscosity (μ_t) with disc opening of 20%, 50%, 100% using two-equation k–ω model (Values in BOLD represent maximum absolute)

% disc opening		α		β		β'		σ_k		σ_ω	
20%	①	0.49	0.39	2.11	**4.41**	0.89	0.78	0.14	0.25	0.03	0.88
	②	0.00	0.00	**0.52**	0.14	0.02	0.32	0.01	0.00	0.00	0.00
	③	6.90	3.23	**8.39**	1.82	3.45	3.94	0.04	0.21	0.47	0.31
	④	0.12	0.43	**4.45**	0.33	0.02	1.96	0.22	0.01	0.10	0.23
50%	①	0.05	0.18	**1.59**	0.53	0.37	1.08	0.05	0.03	0.07	0.03
	②	0.04	0.00	0.02	**0.26**	0.09	0.11	0.02	0.00	0.01	0.01
	③	7.36	5.79	5.76	**7.60**	4.11	0.22	0.08	0.02	0.15	0.40
	④	0.03	0.25	**3.43**	0.12	0.08	2.43	0.26	0.00	0.09	0.01
80%	①	0.10	0.08	0.40	**3.09**	0.65	0.32	0.01	0.04	0.10	0.11
	②	0.00	0.05	**0.46**	0.07	0.05	0.25	0.01	0.00	0.02	0.00
	③	6.50	1.04	1.84	**7.86**	2.32	1.41	0.00	0.29	0.29	0.02
	④	0.01	0.22	**1.76**	0.11	0.07	1.11	0.02	0.02	0.07	0.00

Developing location (5Y)

% disc opening		α		β		β'		σ_k		σ_ω	
20%	①	0.41	0.34	**2.09**	0.70	0.62	0.43	0.03	0.06	0.00	0.05
	②	0.00	0.00	0.06	**0.18**	0.00	0.01	0.00	0.00	0.00	0.00
	③	**6.54**	5.70	1.20	4.10	0.55	1.37	0.00	0.03	0.00	0.01
	④	0.18	0.11	0.25	**1.80**	0.01	0.59	0.04	0.00	0.06	0.03
50%	①	0.06	0.09	**0.94**	0.49	0.18	0.38	0.04	0.03	0.01	0.07
	②	0.01	0.00	0.02	**0.06**	0.02	0.03	0.00	0.00	0.00	0.00
	③	**5.53**	1.65	1.71	4.38	1.20	0.41	0.01	0.03	0.09	0.01
	④	0.03	0.09	**1.62**	0.08	0.05	1.19	0.03	0.00	0.10	0.01
80%	①	1.09	1.17	1.11	**3.13**	0.72	0.41	0.02	0.02	0.05	0.10
	②	0.01	0.01	**0.31**	0.06	0.06	0.18	0.01	0.00	0.01	0.00
	③	**8.41**	6.19	1.08	4.77	1.51	1.34	0.03	0.25	0.29	0.24
	④	0.03	0.23	**2.25**	0.10	0.08	1.58	0.04	0.02	0.19	0.02

Developed location (10Y)

turbulence constants of α and β. At the developing location of 5Y, relatively high turbulence specific dissipation rate is observed, particularly for the low opening of 20%. Extremely high turbulence specific dissipation rates are affected by constant α. On increasing the opening to 100%, the turbulence specific dissipation rate is affected by constant β. At the developed location of 10Y, high turbulence specific dissipation rates are also observed for the high opening of 100%. However, the extremely high turbulence specific dissipation rates are only affected by constant α. Using the two-equation $k-\omega$ model, large discrepancies occur in the developing and developed flow regions with small and large opening angles of the disc, respectively.

Overall, sensitivity is high for numerical calculations close to the area near the valve disc, which is the constriction area in the developing flow region. High sensitivity is also observed in the developed flow region with a large opening angle, using the two-equation turbulence models. Therefore, Numerical checks for calculations involving turbulence parameters should be carried out, particularly focusing on the flow-developed region close to the disc opening angle.

5. CONCLUDING REMARKS

A numerical study of triple-offset butterfly valve with different sizes (300, 400, and 450 mm) was conducted and the effect of the two-equation turbulence models of k–ε, k-ω, and Reynolds stress model was examined in various valve disc-opening cases. The numerical method was validated using the experimentally obtained valve flow test results with various sizes. The turbulence model effect and the consequent flow behavior in the valves was analyzed in different opening of disc. The sensitivity of the turbulence model constants was examined using the 300 mm valve to analyze sensitivity of the turbulence model parameters in the two-equation turbulence models. The main conclusions were as follows:

1. For the validation of numerical calculations, the discrepancy between the numerical and experimental results is decreased with increasing size of the valve. In addition, the RS model shows high level of

numerical prediction accuracy among the turbulence models

2. The flow behavior of the valves revealed the presence of numerous vortices and wake regions when the disc opening of 20%. With 50% disc opening angle, the flow recirculation, secondary flows, and vortex mixing were observed due to the wakes. With 100% disc opening angle, the recirculation and swirling behind the valve decreased as a result of the large area between the disc and the pipe wall
3. Among the turbulence models, the RS model expressed the turbulence effect the most. Among the two-equation turbulence models, the k–ε model showed a high level of turbulence kinetic energy better than the k–ω model. Reynolds normal stress are higher value at the 5Y location than 10Y location indicating that the RS model predicts stresses more accurately near the valve disc region than in other regions.
4. As the valve size and opening angle decreased, the difference between the results increased with the turbulence models. The increase in the difference between the turbulence models was attributed to the decrease in the effective flow region. This decrease resulted in relatively reduced area between the disc and valve wall, leading to increased pressure drop and velocity, which, in turn, increased turbulence.
5. Sensitivity of the turbulence model constants was studied using the sensitivity coefficients for the flow behavior in the 300 mm valve with different disc opening angles. For the two-equation $k-\varepsilon$ model, the flow property most sensitive to the parameters was the turbulence dissipation rate, and it was mainly influenced by the constants C_{1e} and C_{2e}. For the two-equation $k-\omega$ model, the flow property most sensitive to the parameters was also the turbulence specific dissipation rate, and it was mainly affected by the constants α and β.
6. The numerical method adopted in a study can serve as a valuable and versatile tool for future research on various valve systems using different types of valves. the findings of this research have broad applications and can be widely utilized in the engineering design of various valve systems.

FUNDING

This work was funded by the Materials/Parts Technology Development Program (20017575, Development of Applicability Evaluation Technology for Cryogenic Insulation Material and Storage Vessel considering Operating Condition of Hydrogen Commercial Vehicle) funded By the Ministry of Trade, Industry & Energy (MOTIE, Korea)

ACKNOWLEDGEMENTS

This work is supported by the Korea Agency for Infrastructure Technology Advancement (KAIA) grant funded by the Ministry of Land, Infrastructure and Transport (Grant No. RS-2021-KA163348) and in part by a grant from R&D Program (PK2303D4) of the Korea Railroad Research Institute.

CONFLICT OF INTEREST

The authors declare that they have no conflicts of interest.

REFERENCES

Ansys, Inc. "CFX Solver Modelling Guide, Release 15.0." ANSYS CFX-Solver Modeling Guide 15317.November (2013): 724-46. https://www.kth.se/polopoly_fs/1.332104.1600689183!/rn_r15.pdf

Bardina, J. E., Huang, P. G., & Coakley, T. J. (1997). *Turbulence modeling validation, testing, and development.* No. A-976276.

Benton, J., Kalitzin, G., & Gould, A. (1996). *Application of two-equation turbulence models in aircraft design*. 34th Aerospace Sciences Meeting and Exhibit. https://doi.org/10.2514/6.1996-327

Błazik-Borowa, E. (2008). The analysis of the channel flow sensitivity to the parameters of the k–ε method. *International Journal for Numerical Methods in Fluids*, 58, 1257-1286. https://doi.org/10.1002/fld.1808

Błazik-Borowa, E. (2012). The application example of the sensitivity analysis of the solution to coefficients of the k-ε model. *Budownictwo i Architektura*, 10, 53-68. https://doi.org/10.35784/bud-arch.2230

Bottema, M. (1997). Turbulence closure model "constants" and the problems of "inactive" atmospheric turbulence. *Journal of Wind Engineering and Industrial Aerodynamics*, 67, 897-908. https://doi.org/10.1016/S0167-6105(97)00127-X

Chen, Y. S., & Kim, S. W. (1987). *Computation of turbulent flows using an extended k-epsilon turbulence closure model*. No. NAS 1.26, 179204.

Choi, S. W., & Kim, H. S. (2020). Predicting turbulent flows in butterfly valves with the nonlinear eddy viscosity and explicit algebraic Reynolds stress models. *Physics of Fluids*, 32, 085105. https://doi.org/10.1063/5.0006896

Choi, S. W., Seo, H. S., & Kim, H. S. (2021). Analysis of flow characteristics and effects of turbulence models for the butterfly valve. *Applied Sciences*, 11, 6319. https://doi.org/10.3390/app11146319

Colin, E., Etienne, S., Pelletier, D., & Borggaard, J. (2005). Application of a sensitivity equation method to turbulent flows with heat transfer. *International Journal of Thermal Sciences*, 44, 1024-1038. https://doi.org/10.1016/j.ijthermalsci.2005.04.002

Comte-Bellot, G., & Corrsin, S. (1966). The use of a contraction to improve the isotropy of grid-generated turbulence. *Journal of Fluid Mechanics*, 25, 657-682. https://doi.org/10.1017/S0022112066000338

Del Toro, A., M. C. Johnson, & R. E. Spall (2015). Computational fluid dynamics investigation of butterfly valve performance factors. *Journal-American Water Works Association*, 107.5, E243-E254. https://doi.org/10.5942/jawwa.2015.107.0052

Du, X., & Gao, S. (2013). Numerical study of complex turbulent flow through valves in a steam turbine system. *International Journal of Materials, Mechanics and Manufacturing*, 1, 301-305. https://doi.org/10.7763/IJMMM.2013.V1.65

Henderson, A. D., Sargison, J. E., Walker, G. J., & Haynes, J. (2008). A numerical prediction of the hydrodynamic torque acting on a safety butterfly valve in a hydro-electric power scheme. *WSEAS Transactions on Fluid Mechanics*, 1, 218. http://www.wseas.us/e-library/transactions/fluid/2008/MGR-03.pdf

Hrenya, C. M., Bolio, E. J., Chakrabarti, D., & Sinclair, J. L. (1995). Comparison of low Reynolds number k− ε turbulence models in predicting fully developed pipe flow. *Chemical Engineering Science*, 50, 1923-1941. https://doi.org/10.1016/0009-2509(95)00035-4

Huang, C., & Kim, R. H. (1996). Three-dimensional analysis of partially open butterfly valve flows. https://doi.org/10.1115/1.2817795

ISA (2007a). *Standard, control valve capacity test procedures. ISA-S75;* The International Society of Automation: Research Triangle Park, NC, USA. https://webstore.ansi.org/preview-pages/ISA/preview_ANSI+ISA+75.02.01-2008.pdf

ISA (2007b). *Standard, Flow Equations for Sizing Control Valves. ISA-S75*; The International Society of Automation: Research Triangle Park, NC, USA. http://integrated.cc/cse/ISA_750101_SPBd.pdf

Jones, W. P., & Launder, B. E. (1972). The prediction of laminarization with a two-equation model of turbulence. *International Journal of Heat and Mass Transfer*, 15, 301-314. https://doi.org/10.1016/0017-9310(72)90076-2

Kok, J. C. (2000). Resolving the dependence on freestream values for the k-turbulence model. *AIAA Journal*, 38, 1292-1295. https://doi.org/10.2514/2.1101

Launder, B. E., & Sharma, B. I. (1974). Application of the energy-dissipation model of turbulence to the calculation of flow near a spinning disc. *Letters In Heat and Mass Transfer*, 1, 131-137. https://doi.org/10.1016/0094-4548(74)90150-7

Launder, B. E., & Spalding, D. B. (1972). Lectures in mathematical models of turbulence.

Launder, B. E., & Spalding, D. B. (1974). The numerical computation of turbulent flows. *Computer Methods in Applied Mechanics and Engineering*, 3, 269-289. https://doi.org/10.1016/0045-7825(74)90029-2

Lin, C. H., Yen, C. H., & Ferng, Y. M. (2014). CFD investigating the flow characteristics in a triangular-pitch rod bundle using Reynolds stress turbulence model. *Annals of Nuclear Energy*, 65, 357-364. https://doi.org/10.1016/j.anucene.2013.11.023

Lisowski, E., & Filo, G. (2017). Analysis of a proportional control valve flow coefficient with the usage of a CFD method. *Flow Measurement and Instrumentation*, 53, 269-278. https://doi.org/10.1016/0019-0578(95)00023-2

Lisowski, E., & Rajda, J. (2013). CFD analysis of pressure loss during flow by hydraulic directional control valve constructed from logic valves. *Energy Conversion and Management*, 65, 285-291. https://doi.org/10.1016/j.enconman.2012.08.015

Nesbitt, B. (2011). *Handbook of valves and actuators: valves manual international*. Elsevier. https://doi.org/10.1016/B978-1-85617-494-7.X5027-5

Ogawa, K., & Kimura, T. (1995). Hydrodynamic characteristics of a butterfly valve—prediction of torque characteristics. *ISA Transactions*, 34, 327-333.

Park, J. Y., & M. K. Chung (2006). Study on hydrodynamic torque of a butterfly valve. 190-195. https://doi.org/10.1115/1.2137348

Patel, Y. (2010). Numerical investigation of flow past a circular cylinder and in a staggered tube bundle using various turbulence models. https://doi.org/10.1088/1757-899X/383/1/012050

Prieler, R., Demuth, M., Spoljaric, D., & Hochenauer, C. (2015). Numerical investigation of the steady flamelet approach under different combustion environments. *Fuel*, 140, 731-743. https://doi.org/10.1016/j.fuel.2014.10.006

Said, M. M., AbdelMeguid, H. S., & Rabie, L. H. (2016). The accuracy degree of CFD turbulence models for butterfly valve flow coefficient prediction. *American Journal of Industrial Engineering*, 4, 14-20. https://doi.org/10.12691/ajie-4-1-3

Sarkar, A., & So, R. M. C. (1997). A critical evaluation of near-wall two-equation models against direct numerical simulation data. *International Journal of Heat and Fluid Flow*, 18, 197-208. https://doi.org/10.1016/S0142-727X(96)00088-4

Sarkar, T., Sayer, P. G., & Fraser, S. M. (1997). Flow simulation past axisymmetric bodies using four different turbulence models. *Applied Mathematical Modelling*, 21, 783-792. https://doi.org/10.1016/S0307-904X(97)00102-9

Shih, T. H. (1990). *An improved k-epsilon model for near-wall turbulence and comparison with direct numerical simulation.* No. NAS 1.15, 103221.

Shih, T. H., Liou, W. W., Shabbir, A., Yang, Z., & Zhu, J. (1995). A new k-ϵ eddy viscosity model for high reynolds number turbulent flows. *Computers & Fluids*, 24, 227-238. https://doi.org/10.1016/0045-7930(94)00032-T

Srikanth, C., & Bhasker, C. (2009). Flow analysis in valve with moving grids through CFD techniques. *Advances*

in Engineering Software, 40, 193-201. https://doi.org/10.1016/j.advengsoft.2008.04.003

Sun, X., Kim, H. S., Yang, S. D., Kim, C. K., & Yoon, J. Y. (2017). Numerical investigation of the effect of surface roughness on the flow coefficient of an eccentric butterfly valve. *Journal of Mechanical Science and Technology*, 31, 2839-2848. https://doi.org/10.1007/s12206-017-0527-0

Wang, P., & Liu, Y. (2017). Unsteady flow behavior of a steam turbine control valve in the choked condition: Field measurement, detached eddy simulation and acoustic modal analysis. *Applied Thermal Engineering*, 117, 725-739. https://doi.org/10.1016/j.applthermaleng.2017.02.087

Wilcox, D. C. (1998). *Turbulence modeling for CFD*. La Canada, CA: DCW industries. https://doi.org/10.1017/S0022112095211388

Wilcox, D. C. (2008). Formulation of the kw turbulence model revisited. *AIAA Journal*, 46(11), 2823-2838. https://doi.org/10.2514/1.36541

Williams, S., Trembley, J., & Miller, J. P. Flow *Monitoring using flow control device*. U.S. Patent No. 7,092,797, 15 August 2006.

Wu, D., Li, S., & Wu, P. (2015). CFD simulation of flow-pressure characteristics of a pressure control valve for automotive fuel supply system. *Energy Conversion and Management*, 101, 658-665. https://doi.org/10.1016/j.enconman.2015.06.025

Zeng, L., Liu, G., Mao, J., Yuan, Q., Wang, S., Wei, L., & Wang, Z. (2015). A novel numerical simulation method to verify turbulence models for predicting flow patterns in control valves. *Journal of Fluid Science and Technology*, 10, JFST0007-JFST0007. https://doi.org/10.1299/jfst.2015jfst0007